AIP | Journal of Applied Physics

# Analysis of the optical properties of Cu(In1−xGax)3Se5 crystals

M. León, R. Serna, S. Levcenko, G. Gurieva, J. M. Merino et al.

Citation: J. Appl. Phys. **104**, 093507 (2008); doi: 10.1063/1.2986159
View online: http://dx.doi.org/10.1063/1.2986159
View Table of Contents: http://jap.aip.org/resource/1/JAPIAU/v104/i9
Published by the American Institute of Physics.

# Analysis of the optical properties of $Cu(In_{1-x}Ga_x)_3Se_5$ crystals

M. León,[1,a] R. Serna,[2] S. Levcenko,[3] G. Gurieva,[3] J. M. Merino,[1] E. J. Friedrich,[1] and E. Arushanov[1,3]
[1]*Departamento Física Aplicada, Universidad Autónoma de Madrid, C-XII, 28049 Madrid, Spain*
[2]*Laser Processing Group, Instituto de Óptica, CSIC, Serrano 121, 28006 Madrid, Spain*
[3]*Institute of Applied Physics, Academy of Sciences of Moldova, Chisinau MD 2028, Moldova*

(Received 12 June 2008; accepted 29 July 2008; published online 5 November 2008)

Analysis of the optical properties of bulk $Cu(In_{1-x}Ga_x)_3Se_5$ mixed crystals synthesized from the elements as a function of the Ga content is presented. Measurements of the complex dielectric function $\varepsilon(\omega)=\varepsilon_1(\omega)+i\varepsilon_2(\omega)$ were performed at room temperature in the photon energy range of 0.8–4.7 eV using a variable angle of incidence ellipsometer. The spectral dependence of the complex refractive index, the absorption coefficient, and the normal-incidence reflectivity were also derived. The structure observed in the dielectric functions attributed to the interband transitions $E_0$, $E_{1A}$, and $E_{1B}$ has been modeled using a modification of the Adachi's model. The results are in excellent agreement with the experimental data over the entire range of photon energies. The model parameters, including the energies corresponding to the lowest direct gap and higher critical points, have been determined using the simulated annealing algorithm. The values of $E_0$ and $E_{1A}$ are found to increase linearly with the increasing Ga content. © *2008 American Institute of Physics*.
[DOI: 10.1063/1.2986159]

## I. INTRODUCTION

Polycrystalline thin-film solar cells based on $CuInSe_2$ and related materials are among the most promising candidates for terrestrial applications of photovoltaic energy generation. Devices based on $CuIn_{1-x}Ga_xSe_2$ have demonstrated efficiencies up to 19.9%.[1] Several studies showed the existence of an ordered-defect-compound (ODC) surface layer ($CuIn_3Se_5$) onto the $CuInSe_2$ absorber in some high efficiency thin film cells. A similar ODC surface layer is expected to improve the efficiency of the $CuIn_{1-x}Ga_xSe_2$-based solar cells.[2–4] Therefore, a detailed study of the physical properties of ODCs is important to have a better understanding of device operation and further improvement of solar cell performance. However, so far the characteristics of ODCs, especially ODCs solid solutions, have not yet been well determined. Only absorption coefficients were determined for $Cu(In_{1-x}Ga_x)_3Se_5$ (Refs. 4 and 5) and $Cu(In_{1-x}Ga_x)_2Se_{3.5}$ (Ref. 6) thin film alloys by optical transmission data, and the band gap values $E_g$ were estimated.

Spectroscopic ellipsometry (SE) is a high-precision optical technique used to study the optical and electronic properties of semiconductors. Over a wide energy range SE permits to determine their dielectric functions, which are directly related to the electronic energy-band structure of the material studied. More recently, SE studies have been carried out on the $CuIn_2Se_{3.5}$,[7,8] $CuIn_3Se_5$,[9] $CuIn_5Se_8$,[9] $CuGa_3Se_5$,[7,8] and $CuGa_5Se_8$ (Ref. 8) ternary compounds.

In this work, we have measured the ellipsometric spectra of several $Cu(In_{1-x}Ga_x)_3Se_5$ polycrystalline alloys at room temperature in the 0.8–4.7 eV energy range. The modeling of their dielectric functions and optical constants has been performed, and the values for interband transition energies as well as their dependence on composition as a function of the Ga content ($x$) have been obtained.

## II. EXPERIMENTAL METHODS AND ANALYSIS METHODOLOGY

The $Cu(In_{1-x}Ga_x)_3Se_5$ crystals were synthesized from the individual elements with 99.9999% purity in a vacuum sealed quartz tube. This ampoule was introduced in a rocking horizontal furnace that was gently heated to 1100 °C avoiding overpressures and cooled slowly at the rate of 5–10 °C/h. The energy dispersive x-ray (EDAX) microanalysis was used to measure the composition of the samples. The results of such analysis have been gathered in Table I. The composition of samples used in the optical study can be described as $Cu(In_{0.58}Ga_{0.41})_2Se_{3.2}$ (IG1), $Cu_{1.2}(In_{0.61}Ga_{0.39})_3Se_{4.8}$ (IG2), and $Cu(In_{0.33}Ga_{0.69})_3Se_{4.8}$ (IG3). The structural analysis was performed by x-ray diffraction, and it was found that the ingots were polycrystalline single phase presenting tetragonal structures, as shown in Fig. 1. According to Refs. 5 and 6, the values of $E_g$ are practically the same for $Cu(In_{1-x}Ga_x)_2Se_{3.5}$ and $Cu(In_{1-x}Ga_x)_3Se_5$ solid solutions, with a negligible dependence on the Cu and Se contents. This fact permitted to analyze IG1 as a sample with properties similar to those of a film with composition $Cu_{1.5}(In_{0.58}Ga_{0.41})_3Se_{4.8}$. In the following, the analysis has been performed considering all samples belonging to the $Cu(In_{1-x}Ga_x)_3Se_5$ solid solution, and the results have been analyzed as a function of the Ga content.

The optical measurements were performed with a variable-angle spectroscopic ellipsometer at room temperature, in the photon energy range from 0.8 to 4.7eV, and at two incidence angles, $\Phi=60°$ and $\Phi=70°$.[7] In order to re-

[a]Electronic mail: maximo.leon@uam.es.

 

TABLE I. Compositional data of the studied samples carried out by EDAX.

| Samples | Cu at. % | In at. % | Ga at. % | Se at. % | (In+Ga)/Cu | Se/Cu |
|---|---|---|---|---|---|---|
| $Cu(In_{0.58}Ga_{0.41})_2Se_{3.2}$ (IG1) | 16.2 | 18.5 | 13.2 | 52.1 | 1.96 | 3.22 |
| $Cu_{1.2}(In_{0.61}Ga_{0.39})_3Se_{4.8}$ (IG2) | 13.3 | 20.3 | 12.7 | 53.7 | 2.48 | 4.04 |
| $Cu(In_{0.33}Ga_{0.69})_3Se_{4.8}$ (IG3) | 11.3 | 11.3 | 23.3 | 54.1 | 3.06 | 4.79 |

move undesired overlayers formed on the surface, the samples were specially prepared as described in Ref. 10, and hence, a two phase model (atmosphere-sample) was used to analyze the ellipsometry spectra.[10,11] The complex dielectric functions have been determined following Eq. 1 of Ref. 9.

The features observed in the complex dielectric function spectra $\varepsilon=\varepsilon(\hbar\omega)$ have been described in terms of the interband transitions using a modified Adachi's model. This model combines the merits of the standard critical point (CP) and damped harmonic oscillator models[12] and has been successfully applied to model the dielectric functions of several *III–V*, *I–III–VI*$_2$, and ODC compounds, as well as their optical constants.[7–10,12–16] The modified Adachi model has been extensively explained in our previous work in Ref. 7. In this model the complex dielectric function is described by the sum of two terms $\varepsilon_0(E)$ and $\varepsilon_1(E)$, corresponding, respectively, to the one-electron contributions at the $E_{0\alpha}$ and $E_{1\beta}$ CPs, where $\alpha=\alpha$, *b*, *c* refers to the triple valence band splitting level in chalcopyrites and $\beta=A$, *B* refers to different energy transitions after the main one. It is worth mentioning that in our case, splitting among the $E_0$ CPs is not observed and they have been treated as a single degenerate point.

In order to obtain the model parameters, the simulated annealing (SA) algorithm has been used[15–17] through the minimization of the following objective function:

$$F=\sum_{i=1}^{N}\left(\left|\frac{\varepsilon_1(\omega_i)}{\varepsilon_1^{\mathrm{expt}}(\omega_i)}-1\right|+\left|\frac{\varepsilon_2(\omega_i)}{\varepsilon_2^{\mathrm{expt}}(\omega_i)}-1\right|\right)^2, \quad (1)$$

where $\varepsilon_1^{\mathrm{expt}}(\omega_i)$, $\varepsilon_1(\omega_i)$ and $\varepsilon_2^{\mathrm{expt}}(\omega_i)$, $\varepsilon_2(\omega_i)$ are, respectively, the experimental and calculated values of the real and imaginary parts of complex dielectric function at $\omega_i$ point, and the summation is performed over the available range of experimental points. Such model has also shown good agreement with the experimental data for *III–V* materials and ODC compounds.[7–9,13–16]

## III. RESULTS AND DISCUSSIONS

The experimental pseudodielectric functions $\varepsilon(\omega)=\varepsilon_1(\omega)+i\varepsilon_2(\omega)$ of the samples IG1, IG2, and IG3 are presented in Fig. 2. The spectra corresponding to the ternary end compounds are also plotted. The line shapes of $\varepsilon_1(\omega)$ and $\varepsilon_2(\omega)$ in all our samples are dominated by two distinct peaks. In the spectral range under consideration, the line shape of the dielectric function is determined by the electronic band structure, and the observed structures usually correspond to transitions at high-symmetry points or lines in the Brillouin zone. These CPs are characterized by a high joint density of states combined with nonvanishing transition matrix elements. The dielectric function is considered as a sum of the contributions from all allowed transitions at CPs.[18,19]

The Adachi model was applied to calculate the dielectric function as well as the optical constants of the studied crystals. The resulting analytical lines in Fig. 3 have been obtained from the fits of the experimental data considering 3*D*-type CPs in the lowest energy region $E_0$ and 2*D* type in the intermediate and high energy region $E_1$. The *A*, *B*, *E*, and

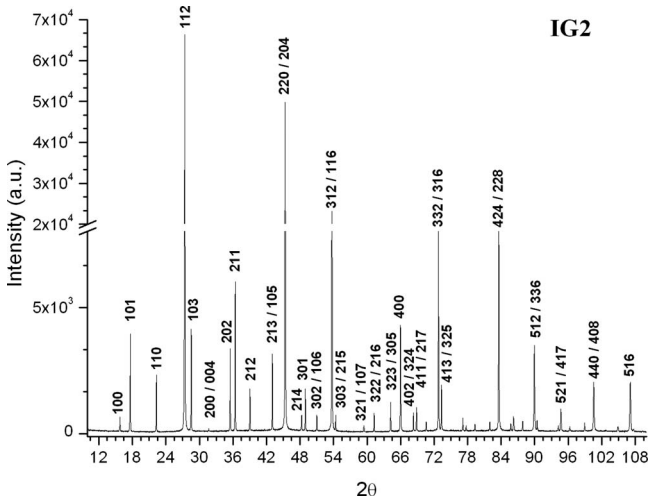


FIG. 1. X-ray powder diffraction diagram of the IG2 sample. The indexing is depicted for all reflections below $2\theta=70°$; for higher $2\theta$ values, indexing is omitted for clarity.

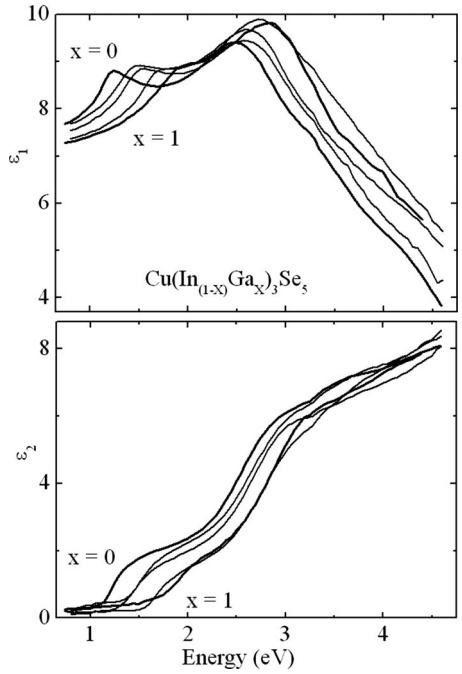


FIG. 2. Real $\varepsilon_1$ and imaginary $\varepsilon_2$ parts of the dielectric function vs energy for $Cu(In_{1-x}Ga_x)_3Se_5$ alloys. The spectra corresponding to the ternary end compounds are plotted with thicker lines.

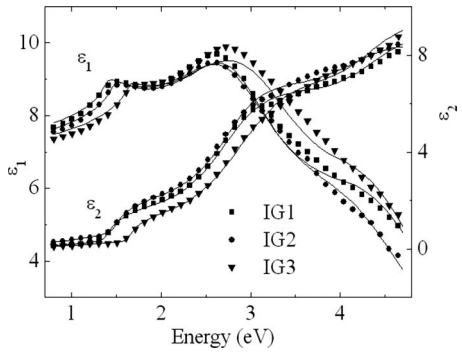


FIG. 3. Real $\varepsilon_1$ and imaginary $\varepsilon_2$ parts of the dielectric function vs energy for IG1, IG2, and IG3 samples. Solid squares, circles, and triangles represent the experimental data, while the solid lines correspond to the theoretical fits of these data.

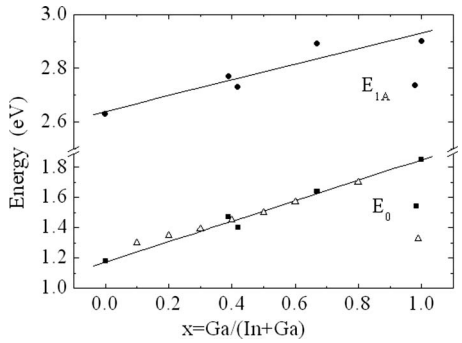


FIG. 4. Compositional dependence of the $E_0$ and $E_1(A)$ in $Cu(In_{1-x}Ga_x)_3Se_5$ alloys. Solid squares and circles represent data after this work, while open triangles correspond to data after Negami *et al.* (Ref. 5).

Γ model parameters calculated using the SA algorithm are given in Table II. The lowest $E$ value observed in the region below 1.7 eV corresponds to the fundamental energy gap value $E_0=E_g$, well distinguished for each studied sample (Figs. 2 and 3). Besides, a second $E_{1A}$ and a third $E_{1B}$ energy thresholds appear in the region between 2.5 and 4.5 eV (Table II).

An excellent agreement between our calculations and the $\varepsilon_1^{expt}(\omega)$ and $\varepsilon_2^{expt}(\omega)$ experimental data has been observed for all studied samples. The fit with the adjustable parameters given in Table II is shown in Fig. 3. As an indication of the accuracy with respect to the experimental values, the relative errors have been calculated, lying in the 2%–2.9% and 3.2%–5.7% ranges for the real and the imaginary parts, respectively (Table II).

Band structure calculations are not available for $Cu(In_{1-x}Ga_x)_3Se_5$; however, the structure of the fundamental absorption edge of chalcopyrites is well understood.[20] These crystals are semiconductors with a direct fundamental gap at the Brillouin-zone center Γ. Based on the band structure calculations from Jaffe and Zunger[21] for the ternary end compounds and relating the observed transitions to those of the binary zinc-blend analogs, the main transitions that contribute to $\varepsilon(\omega)$ could be assigned to CPs at the Brillouin-zone center Γ and edge points $N$ and $T$. The labeling of these transitions is described in Ref. 22 and is related to the standard zinc-blend notation.

The band structure calculations obtained for $CuInSe_2$ (CIS) and $CuGaSe_2$ (CGS) (Ref. 20) have also been used to identify the energy values observed in $Cu(In_{1-x}Ga_x)_3Se_5$. The energy threshold of the fundamental absorption edge $E_0=E_g$, well identified in the spectra of studied materials (Figs. 2 and 3), can be related to an electronic transition at the Γ point. The estimated values of $E_g$ at room temperature, 1.47 eV($x$=0.39), 1.4 eV($x$=0.41), and 1.64 eV($x$=0.69) for the samples belonging to the $Cu(In_{1-x}Ga_x)_3Se_5$ solid solutions, are in the range between those previously determined for the two ternary end compounds, $CuIn_3Se_5$ (Ref. 9) and $CuGa_3Se_5$.[7,8] Besides, these values are in an excellent agreement with those reported for $Cu(In_{1-x}Ga_x)_3Se_5$ (Ref. 5) and $Cu(In_{1-x}Ga_x)_2Se_{3.5}$ (Ref. 6) films with the same content of Ga (value of $x$), as shown in Fig. 4.

In the region between 2.5–4.5 eV, two transitions, named as $E_{1A}$ and $E_{1B}$, have also been observed. We have assumed that they can be related to $N$-type transitions after Refs. 10 and 22, where ellipsometric data for CIS and CGS compounds were analyzed. The measured energy separation between these two transitions corresponds to the crystal-field

TABLE II. Model parameter values.

| Parameters | Samples | | | | | | | | | |
|---|---|---|---|---|---|---|---|---|---|---|
| | **I35S** [a] | | **IG1** | | **IG2** | | **IG3** | | **G35B**[b] | |
| $A$ ($eV^{1.5}$) | 4.20 | | 5.89 | | 6.02 | | 5.98 | | 7.40 | |
| $E_0$ (eV) | 1.18 | | 1.40 | | 1.47 | | 1.64 | | 1.85 | |
| Γ (eV) | 0.005 | | 0.038 | | 0.031 | | 0.019 | | 0.043 | |
| $B_{1A}$ (eV) | 2.95 | | 2.69 | | 3.11 | | 2.60 | | 2.48 | |
| $E_{1A}$ (eV) | 2.63 | | 2.73 | | 2.77 | | 2.90 | | 2.90 | |
| $\Gamma_{1A}$ | 0.41 | | 0.40 | | 0.43 | | 0.42 | | 0.32 | |
| $\alpha$ | 0.03 | | 0.12 | | ⋯ | | 0.20 | | 0.25 | |
| $B_{1B}$ (eV) | 3.92 | | 3.97 | | 3.50 | | 3.99 | | 3.7 | |
| $E_{1B}$ (eV) | 4.13 | | 4.43 | | 4.22 | | 4.39 | | 4.24 | |
| $\Gamma_{1B}$ (eV) | 0.87 | | 0.69 | | 0.749 | | 0.64 | | 0.73 | |
| | $\varepsilon_2$ | $\varepsilon_1$ | $\varepsilon_2$ | $\varepsilon_1$ | $\varepsilon_2$ | $\varepsilon_1$ | $\varepsilon_2$ | $\varepsilon_1$ | $\varepsilon_2$ | $\varepsilon_1$ |
| Error | 4.2% | 2.2% | 3.7% | 2.9% | 3.2% | 0.7% | 5.7% | 2.0% | 3.8% | 1.2% |

[a]Data taken from our work in Ref. 9.
[b]Data taken from our work in Ref. 7.

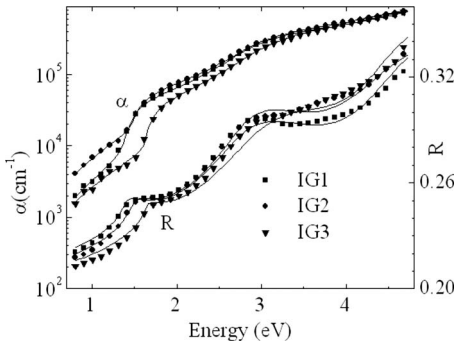


FIG. 5. Experimental (solid squares, circles, and triangles) and theoretically calculated data using the Adachi model and the SA algorithm (solid lines) spectral dependences of the absorption coefficient $\alpha$ and the normal-incidence reflectivity $R$ for IG1, IG2, and IG3 samples.

splitting of the valence band at the $N$ point in the Brillouin zone. In the present work, the crystal-field splitting at the $N$ point was found to lie between 1.5–1.7 eV, close to that (1.3–1.5 eV) estimated for $CuGa_3Se_5$ (Refs. 7 8) and $CuIn_3Se_5$.[9]

As it can be observed in Fig. 4, our results indicate a linearity in the compositional dependence of $E_0$ and $E_{1A}$, as well as some scattering in the $E_{1B}$ values lying around $4.30 \pm 0.15$ eV (Table II). The exact character of the variation in $E_{1B}$ versus the Ga content cannot be easily determined because such variation is quite small (about $\pm 4\%$) and the accuracy in the determination of the $E_{1B}$ value is not high enough.

The optical parameters of interest, namely, the complex refractive index $n^*$, the normal-incidence reflectivity $R$, and the absorption coefficient $a$, have been computed using well known mathematical expressions (see Eqs. 5–7 in Ref. 7). The spectral dependences of $a$, $R$, the real refractive index $n$, and the extinction coefficient $k$ from the experimental data, as well as the calculated ones using the Adachi model and the SA algorithm for the three intermediate samples, are plotted in Figs. 5 and 6. Good agreement is observed for all the studied samples, and the obtained values of the interband CP parameters (strength, threshold energy, and broadening) are given in Table II. All these optical spectra were found to reveal distinct structures at these points.

The experimental refractive index $n$ data have also been

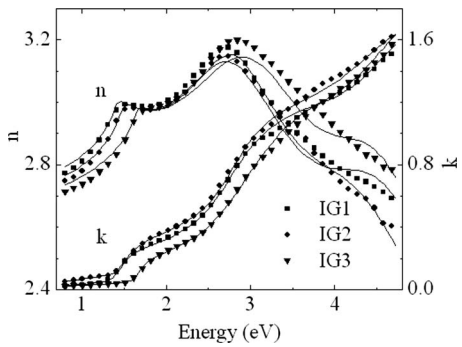


FIG. 6. Experimental (solid squares, circles, and triangles) and theoretically calculated data using the Adachi model and the SA algorithm (solid lines) spectral dependence of the real refraction index $n$ and the extinction coefficient $k$ for IG1, IG2, and IG3 samples.

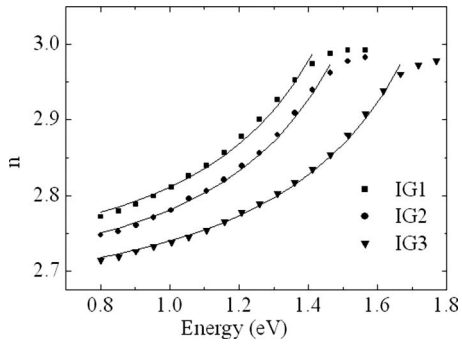


FIG. 7. Real refractive index $n$ vs photon energy for IG1, IG2, and IG3 samples. The solid line shows the calculated result after Eq. (2). Solid squares, circles, and triangles represent the experimental data.

analyzed in the nonabsorbing region (0.8–1.167 eV) using a simple theoretical model, namely, the first-order Sellmeier equation[7–9,14]

$$n^2(\lambda) = A + \frac{\lambda^2}{\lambda^2 - B}, \tag{2}$$

where $A$ and $B$ are the fitting parameters. The solid line in Fig. 7 represents the fitting of Eq. (2) to the experimental data. The values of the fitting parameters $A$ and $B$ are equal to 6.48, 0.46; 6.34, 0.43; and 6.22, 0.34 for IG1, IG2, and IG3 samples, respectively.

As $\lambda \to \infty$, the electronic contribution to the dielectric function approaches the limiting value $\varepsilon_\infty$, i.e., the high-frequency dielectric constant. The value of $\varepsilon_\infty = n^2$ $(\lambda \to \infty) = A + 1$ is about 7.34, 7.48, and 7.22 for the $Cu(In_{1-x}Ga_x)_3Se_5$ intermediate samples with $x = 0.39$, 0.41, and 0.69, respectively. The reported values for $CuIn_3Se_5$ and $CuGa_3Se_5$ are $\varepsilon_\infty = 7.2 - 7.4$.[7,9]

## IV. CONCLUSIONS

The optical properties of several $Cu(In_{1-x}Ga_x)_3Se_5$ intermediate samples have been studied by SE. The spectral dependences of the real and imaginary parts of the complex dielectric function for several $Cu(In_{1-x}Ga_x)_3Se_5$ samples with $x$ in the 0.39–0.69 range are modeled in the 0.8–4.7 eV photon energy range using a modification of Adachi's model for the complex dielectric function of semiconductors and the SA algorithm. An excellent agreement with the experimental data is obtained and the model parameters (strength, threshold energy, and broadening) have been determined. It has also been shown that both the fundamental gap $E_g$ and the $E_{1A}$ values increase linearly with the Ga content. In addition, the complex refractive index, the extinction and absorption coefficients, and the normal-incidence reflectivity have been computed. Both spectral dependences of the optical functions and the CP analysis are expected to be useful in studies of solar cells and other heterostructures that contain these materials.

## ACKNOWLEDGMENTS

Financial support from Comunidad Autónoma de Madrid government FOTOFLEX under Project No. S-0505/ENE/0123, from the Spanish government MEC under Project No.

MAT2003-01490, and from Belarus-Moldova under Project No. 08.820.05.14BF are acknowledged. One of us (S.L.) would like to thank CRDF-MRDA (Project No. MYSSP-1402) for financial support.

[1]I. Repins, M. A. Contreras, B. Egaas, C. DeHart, J. Scharf, C. L. Perkins, B. To, and R. Noufi, Prog. Photovoltaics **16**, 235 (2008).
[2]D. Schmid, M. Ruckh, F. Granwald, and H. W. Schock, J. Appl. Phys. **73**, 2902 (1993); L. Stolt, J. Hedstrom, J. Kessler, M. Puch, K. O. Velthaus, and H. W. Schock, Appl. Phys. Lett. **62**, 597 (1993).
[3]H. Z. Xiao, L. Yang Chung, and A. Rockett, J. Appl. Phys. **76**, 1503 (1994).
[4]G. Marín, S. Tauleigne, S. M. Wasim, R. Guevara, J. M. Delgado, C. Rincón, A. E. Mora, and G. Sánches Pérez, Mater. Res. Bull. **33**, 1057 (1998).
[5]T. Negami, N. Kohara, M. Nishitani, T. Wada, and T. Hirao, Appl. Phys. Lett. **67**, 825 (1995).
[6]T. Tanaka, N. Tanahashi, T. Yamaguchi, and A. Yoshida, Sol. Energy Mater. Sol. Cells **50**, 13 (1998).
[7]M. León, R. Serna, S. Levcenko, A. Nateprov, A. Nicorici, J. M. Merino, and E. Arushanov, J. Appl. Phys. **101**, 013524 (2007).
[8]M. León, S. Levcenko, A. Nateprov, A. Nicorici, M. Merino, R. Serna, and E. Arushanov, J. Phys. D **40**, 740 (2007); M. León, S. Levcenko, A. Nateprov, A. Nicorici, J. M. Merino, E. J. Friedrich, R. Serna, and E. Arushanov, J. Appl. Phys. **102**, 113503 (2007).
[9]M. León, R. Serna, S. Levcenko, A. Nicorici, J. M. Merino, E. J. Friedrich, and E. Arushanov, J. Appl. Phys. **103**, 103503 (2008).
[10]M. I. Alonso, M. Garrida, C. A. Durante Rincon, and M. Leon, J. Appl. Phys. **88**, 5796 (2000); J. G. Albornoz, R. Serna, and M. León, *ibid.* **97**, 103515 (2005).
[11]R. M. A. Azzam and N. M. Bashara, *Ellipsometry and Polarized Light*, 1st ed. (North-Holland, Amsterdam, 1977).
[12]H. Y. Deng and N. Dai, Phys. Rev. B **73**, 113102 (2006).
[13]T. Kawashima, S. Adachi, H. Miyake, and K. Sugiyama, J. Appl. Phys. **84**, 5202 (1998).
[14]T. Kawashima, H. Yoshikawa, S. Adachi, S. Fuke, and K. Ohtsuka, J. Appl. Phys. **82**, 3528 (1997).
[15]A. B. Djurisic and E. Herbert Li, J. Appl. Phys. **85**, 2848 (1999).
[16]A. B. Djurisic and E. H. Li, Appl. Phys. A: Mater. Sci. Process. **A73**, 189 (2001).
[17]A. Corana, M. Marchesi, C. Martini, and S. Ridella, ACM Trans. Math. Softw. **13**, 262 (1987).
[18]M. Cardona, in *Solid State Physics*, edited by F. Seitz, D. Turnbell, and H. Ehrenreich (Academic, New York, 1969).
[19]D. E. Aspnes, in *Handbook on Semiconductors*, edited by T. S. Moss (North-Holland, Amsterdam, 1980), Vol. II, pp. 109–154.
[20]J. L. Shay and J. H. Wernick, *Ternary Chalcopyrite Semiconductors: Growth, Electronic Properties, and Applications* (Pergamon, Oxford, 1975).
[21]J. E. Jaffe and A. Zunger, Phys. Rev. B **28**, 5822 (1983).
[22]M. I. Alonso, K. Wakita, J. Pascual, M. Garriga, and N. Yamamoto, Phys. Rev. B **63**, 075203 (2001).